Cofilin/ADF is required for retinal elongation and morphogenesis of the *Drosophila* rhabdomere

Hung Pham, Hui Yu, Frank A. Laski *

Department of Molecular Cell and Developmental Biology, and Molecular Biology Institute, University of California at Los Angeles, Los Angeles, CA 90095, USA

ABSTRACT

Drosophila photoreceptors undergo marked changes in their morphology during pupal development. These changes include a five-fold elongation of the retinal cell body and the morphogenesis of the rhabdomere, the light sensing structure of the cell. Here we show that *twinstar* (*tsr*), which encodes *Drosophila* cofilin/ADF (actin-depolymerizing factor), is required for both of these processes. In *tsr* mutants, the retina is shorter than normal, the result of a lack of retinal elongation. In addition, in a strong *tsr* mutant, the rhabdomere structure is disorganized and the microvilli are short and occasionally unraveled. In an intermediate *tsr* mutant, the rhabdomeres are not disorganized but have a wider than normal structure. The adherens junctions connecting photoreceptor cells to each other are also found to be wider than normal. We propose, and provide data supporting, that these wide rhabdomeres and adherens junctions are secondary events caused by the inhibition of retinal elongation. These results provide insight into the functions of the actin cytoskeleton during morphogenesis of the *Drosophila* eye.

© 2008 Elsevier Inc. All rights reserved.

Introduction

Neurons have evolved striking and elaborate shapes that are essential for their function. For example, photoreceptors not only have extended axons that connect the retina to the brain, but also form an intricate sensory region composed of layers of folded membranes that are used to package high concentrations of rhodopsin. In the vertebrate rod, this sensory region is called the outer segment and is composed of modified cilia, having a microtubule base. In *Drosophila*, the sensory region is the rhabdomere, which has an actin-based microvilli structure. Understanding how photoreceptors obtain these intricate shapes is crucial to understanding how they develop. There is an extensive literature describing the mechanisms by which growth cones migrate and extend axons, but much less is known about the morphogenetic mechanisms used by outer segments and rhabdomeres to form their complex structures. To study this issue further, we have analyzed the role of actin cytoskeleton proteins during the formation of the rhabdomere.

The *Drosophila* adult compound eye is composed of approximately 800 identical facets called ommatidia, each of which functions as an independent visual unit (Ready et al., 1976; Wolff and Ready, 1991). This uniformity in structure is seen most clearly in sections through the ommatidia, displaying the precise trapezoidal pattern of the rhabdomeres. The development and differentiation of cells of the eye have been studied in great detail (Moses, 2002). In early 3rd instar larvae, the eye disc is a monolayer of undifferentiated cells. At this time, a wave of development occurs, with the progression of the morphogenetic furrow across the eye disc. As the furrow progresses, cells differentiate into photoreceptor cells, followed by the differentiation of the accessory cells during the early pupal stage (Cagan and Ready, 1989). By 60 h after pupal formation, all the cells of the ommatidia have taken on their identities and start to mature, which includes a five-fold increase in length along the optical axis (Fig. 1A; Longley and Ready, 1995). During this maturation, the rhabdomere forms at the apical surface of the photoreceptor cells, then as the apical surface pivots 90° and expands along the visual axis of the cell, the rhabdomere also extends the full length of this axis (Fig. 1A).

Understanding how a neuron changes shape requires an understanding of how the actin cytoskeleton is altered during development. The mechanisms are best understood during actin-based cell motility events such as the migration of a growth cone (Bamburg et al., 1999; Maskery and Shinbrot, 2005; Pollard et al., 2000; Pollard and Borisy, 2003). Cell migration is initiated when an extracellular stimulus activates the Wasp/Scar proteins (Bi and Zigmond, 1999; Machesky and Cooper, 1999), which in turn bind and activates the Arp2/3 complex of proteins, initiating actin polymerization at the membrane boundary (Blanchoin et al., 2000; Higgs and Pollard, 1999). This polymerization results in a growing web of actin filaments at the leading edge of the cell that "pushes" the membrane forward. The alpha and beta Capping Proteins bind to the ends of filaments, terminating their elongation and directing growth to other filaments (Carlier and Pantaloni, 1997). A limiting

* Corresponding author.
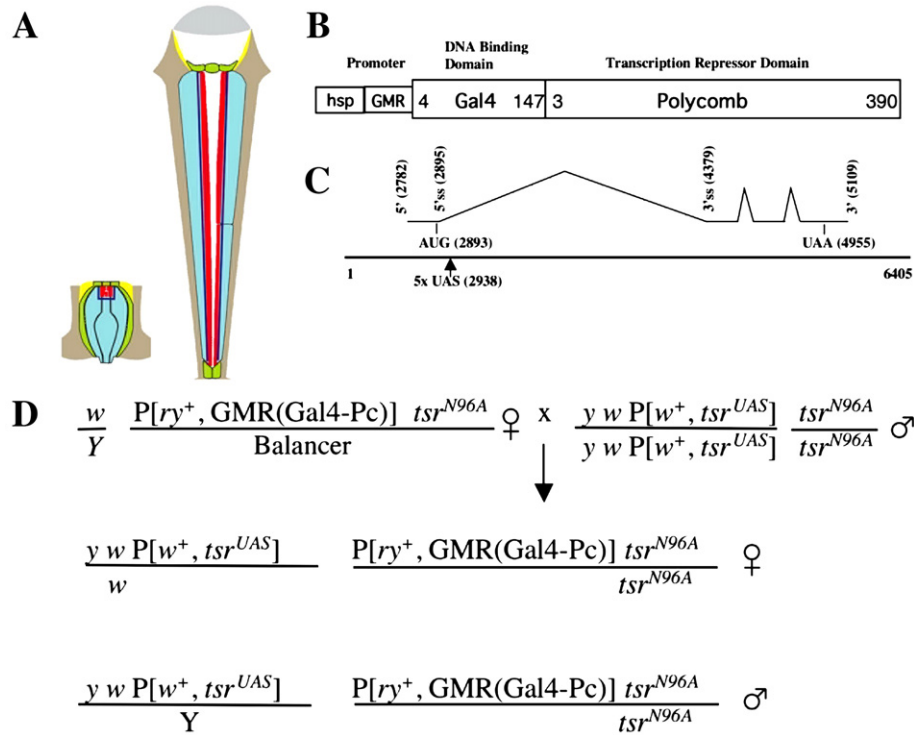E-mail address: laski@mbi.ucla.edu (F.A. Laski).

Fig. 1. (A) The diagram shows the structure of a mid-pupal (left) and adult (right) ommatidium. The adult ommatidium is longer, the result of a five-fold elongation during pupal development. As the photoreceptor cells elongate, the rhabdomeres (red) and adherens junctions (dark blue) elongate with the cells. This drawing was modified from Tepass and Harris (2007). (B) P[ry^+; GMR(Gal4-Pc)] contains the eye specific GMR promoter (Ellis et al., 1993; Moses and Rubin, 1991) driving expression of the Gal4-Pc hybrid protein, which encodes the DNA binding domain of Gal4 (amino acids 4–147) and the repressor domain of Polycomb (amino acids 3–390). The construct also contains the heat shock inducible hsp70 promoter adjacent to the GMR promoter. (C) P[w^+; tsr^{UAS}] contains the tsr 6.4 kb genomic rescue fragment, into which a cassette containing 5 copies of the Gal4 UAS DNA binding site was inserted. P[w^+; tsr^{UAS}] is capable of completely rescuing a tsr null mutation. Base pair positions within the 6.4 kb rescue construct are shown. (D) Genetic cross used to generate the tsr RS mutant flies. TSTL, the compound CyO, TM6B Tb chromosome was used as a balancer.

factor in filament growth is monomeric G-actin, which is at low concentrations in stationary cells (Pantaloni et al., 2001). To initiate cell movement, the G-actin concentration is increased by depoly-merizing F-actin behind the leading edge (Pollard and Borisy, 2003). This turnover and reuse is referred to as actin treadmilling and is stimulated by cofilin/ADF (Pantaloni et al., 2001). All members of the cofilin/ADF family are small actin-binding proteins (13–19 kDa) that bind both F- and G-actin. When cofilin/ADF binds F-actin, a twist is induced in the actin filament structure, which is thought to enhance depolymerization (Bamburg et al., 1999; McGough et al., 1997) and produces a 25-fold increase in the dissociation rate in an *in vitro* system (Carlier, 1998). Recent work has shown that cofilin/ADF is multi-functional, for instance in addition to stimulating cell motility by increasing the concentration of G-actin, it can also sever F-actin at the leading edge, creating more ends and stimulating new rounds of actin polymerization (Wang et al., 2007). Cofilin/ADF is inactivated by phosphorylation of a conserved N-terminal Serine by LIM kinase (Arber et al., 1998; Yang et al., 1998), whereas *slingshot* (*ssh*) encodes a phosphatase that removes the phosphate and activates cofilin/ADF (Niwa et al., 2002).

Cofilin/ADF activity is required for survival in *Drosophila*, as a null mutation in *twinstar* (*tsr*), the *Drosophila* homologue of cofilin/ADF, has a lethal phenotype (Gunsalus et al., 1995). Flies homozygous for a hypomorphic allele of *tsr* displayed cytokinesis defects in both meiosis and mitosis (Gunsalus et al., 1995). A cell motility requirement for *tsr* was demonstrated by showing that *tsr* is required for the cell rearrangements needed for the formation of terminal filaments during ovary morphogenesis, and for the migration of border cells during oogenesis (Chen et al., 2001). These results show that cofilin/ADF is an important regulator of actin-based cell motility during *Drosophila* development.

In this paper, we develop a new type of conditional sensitive allele of *tsr* called a repressor sensitive mutation. Using this mutation, we show that *tsr* activity is required for retinal cell elongation and for the proper morphogenesis of the rhabdomere. In addition, we show that rhabdomeres and adherens junctions undergo abnormal widening in a *tsr* mutant, and we present a model that these mutant phenotypes are secondary events due to the lack of retinal cell elongation.

Results

Construction of tsr repressor sensitive mutations

Strong *tsr* mutations have a recessive lethal phenotype (Gunsalus et al., 1995), dying as first larval instars, making direct study of the role of *tsr* during eye development difficult. Increasing the difficulty is the requirement of *tsr* for cytokinesis (Gunsalus et al., 1995), limiting the use of the FLP/FRT somatic recombination technique. To bypass these obstacles, we use a repressor sensitive (RS) mutation, which allows the activity of *tsr* to be inhibited by the conditional expression of a transcriptional repressor. A cassette containing five Gal4 UAS binding sites was inserted into the first intron of *tsr* (Fig. 1C) within the 6.4 kb *tsr* genomic rescue fragment in a P element construct, and transformed into flies. We found that the P[w^+; tsr^{UAS}] transformants can rescue the $tsr^{Δ96}$ null mutation, indicating that the insertion of the UAS cassette did not inhibit the *tsr* activity of the rescue construct. The P[w^+; tsr^{UAS}] construct was then crossed to a construct that expresses Gal4-Pc, a hybrid protein containing the DNA binding domain of Gal4 fused to the transcriptional repressor domain of Polycomb (Muller, 1995) (Fig. 1B). It had previously been shown that the Gal4-Pc fusion protein could inhibit the expression of a mini-*white* gene that was within a P element

construct that also contained a UAS cassette (Muller, 1995). Here we asked whether Gal4-Pc could turn off the expression of *tsr* and cause a *tsr* mutant phenotype, and found that it could.

Flies homozygous for *tsr^{Δ96}* and that have one copy each of P[w^+; tsr^{UAS}] and P[ry^+; GMR(Gal4-Pc)] were isolated (Fig. 1D). These flies were viable because P[w^+; tsr^{UAS}] can rescue the *tsr^{Δ96}* null mutation. However, the eyes of these flies had defects due to the expression of Gal4-Pc from the eye specific GMR promoter, which represses the expression of *tsr^{UAS}* resulting in a rough eye phenotype (Figs. 2A–H). Expression of Gal4-Pc in a wild type background causes no mutant phenotype (data not shown), therefore the rough eye phenotype is the result of a reduction of *tsr* activity. We tested two different P[w^+; tsr^{UAS}] insertions on the X chromosome and two different P[ry^+; GMR(Gal4-Pc)] insertions on the 2nd chromosome, and found position effect differences in the severity of the phenotype. Flies with the P[ry^+; GMR(Gal4-Pc)]1 insert had a weaker phenotype than flies with the P[ry^+; GMR(Gal4-Pc)]2 insert, suggesting that the latter expresses Gal4-Pc at a higher concentration. P[w^+; tsr^{UAS}]1 flies had a weaker mutant phenotype than P[w^+; tsr^{UAS}]2, suggesting the former either expresses *tsr* at a higher level, or is less susceptible to Gal4-Pc repression. In addition, females had a more severe phenotype than males, likely the result of dosage compensation of the P[w^+; tsr^{UAS}] construct on the X chromosome, where *tsr* is likely transcribed at twice the rate in males. These variations provide a phenotypic series of increasing severity in the adult eye (Figs. 2A–H). Flies within each genotypic class had similar phenotypes with little variation among siblings of the same genotype. In addition to roughness, black patches of dead necrotic cells were also seen.

The P[ry^+; GMR(Gal4-Pc)] construct has a functional hsp70 promoter (Fig. 1B) that is capable of inducing the expression of Gal4-Pc in many tissues. Heat shock induced overexpression of Gal4-Pc in embryos containing the P[ry^+; GMR(Gal4-Pc)] construct is lethal, but overexpression from the larval stages onward had no significant effect on development or viability (data not shown). However, in the P[w^+; tsr^{UAS}] tsr^{Δ96} background (Fig. 1D), repeated overexpression of Gal4-Pc by heat shock from first instar larvae was lethal at the pupal stage, likely the result of Gal4-Pc binding the UAS sites within the *tsr^{UAS}* construct and repressing transcription in many tissues. Initiating Gal4-Pc overexpression at a later stage (third instar larvae) resulted in viable flies with a large assortment of visible developmental defects, including abnormal wing and bristle phenotypes (Supplementary Fig. 1).

twinstar RS mutations inhibit retinal cell elongation

To study the *tsr* RS phenotype, mutant eyes were fixed and sectioned for histological analysis. It was quickly noticed that the *tsr* RS mutant retinas were not as thick as wild type. To verify this, horizontal sections were analyzed. The retina of the Gal4-Pc expressing control was wild type in thickness (Fig. 3A) whereas the retinas of the weakest tsr RS mutant (Fig. 3B) and the strongest (Fig. 3C) were significantly thinner than the control, indicating a requirement for *tsr* during the five-fold elongation of retinal cells. In the stronger *tsr* RS mutants, a defect in the optic lobe is also seen, as there is no clearly defined lamina in the mutant (Fig. 3C). Lamina formation requires innervation from the photoreceptor cells (Kunes
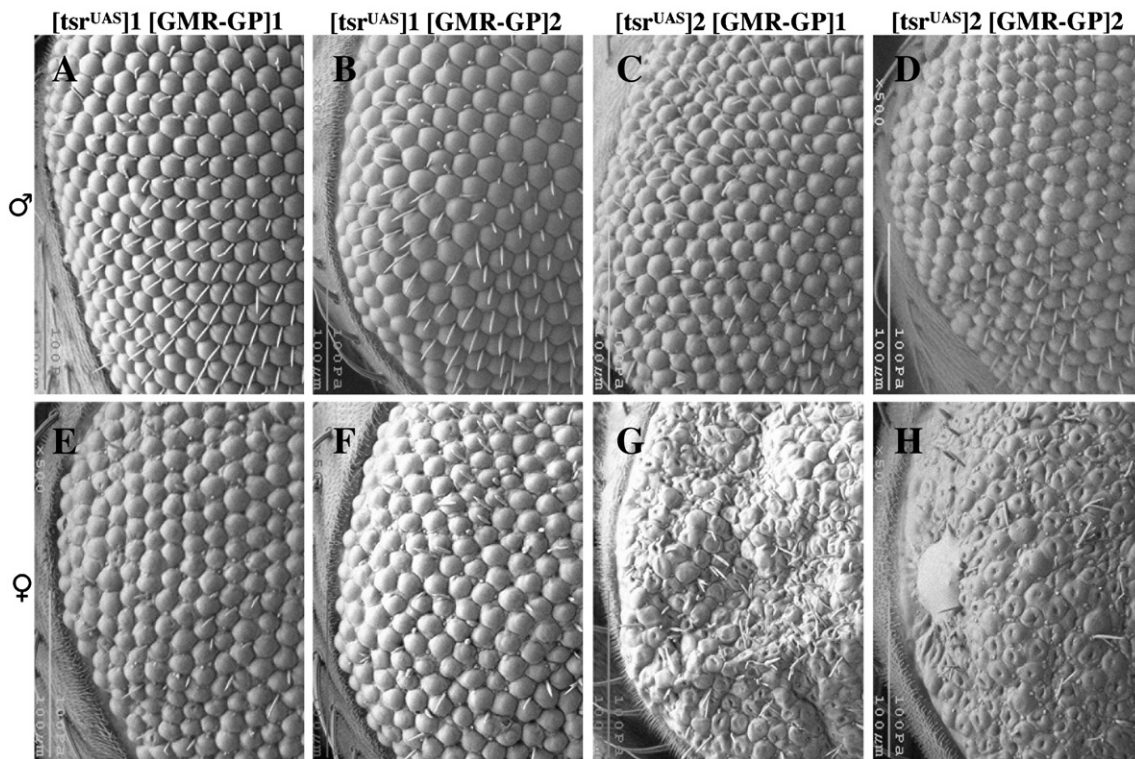

Fig. 2. A phenotypic series of *tsr* RS eye mutants is seen in the scanning electron micrographs of 1 day old adults. The flies are homozygous for the *tsr* null allele *tsr^{Δ96}* but are viable and healthy because they contain the P[w^+, tsr^{UAS}] genomic rescue construct on the X chromosome. These flies also have a construct which expresses Gal4-Polycomb (GP) from the GMR eye specific promoter. Gal4-Pc will bind to the UAS sites in P[w^+, tsr^{UAS}] and inhibit expression of *tsr^{UAS}*. Two different P[w^+, tsr^{UAS}] inserts on the X chromosome (insert 1 and 2) and two different P[ry^+; GMR(Gal4-Pc)] inserts on the second chromosome (inserts 1 and 2) were analyzed and found to have position effect differences. Females were found to have a more severe phenotype than males of the same genotype, likely the result of dosage compensation of P[w^+, tsr^{UAS}] on the X chromosome. The genotypes are: (A) *y w* P[w^+, tsr^{UAS}]1/Y, P[ry^+; GMR(Gal4-Pc)]1 tsr^{N96A}/tsr^{N96A}; (B) *y w* P[w^+, tsr^{UAS}]1/Y, P[ry^+; GMR(Gal4-Pc)]2 tsr^{N96A}/tsr^{N96A}; (C) *y w* P[w^+, tsr^{UAS}]2/Y, P[ry^+; GMR(Gal4-Pc)]1 tsr^{N96A}/tsr^{N96A}; (D) *y w* P[w^+, tsr^{UAS}]2/Y, P[ry^+; GMR(Gal4-Pc)]2 tsr^{N96A}/tsr^{N96A}; (E) *y w* P[w^+, tsr^{UAS}]1/w, P[ry^+; GMR(Gal4-Pc)]1 tsr^{N96A}/tsr^{N96A}; (F) *y w* P[w^+, tsr^{UAS}]1/w, P[ry^+; GMR(Gal4-Pc)]2 tsr^{N96A}/tsr^{N96A}; (G) *y w* P[w^+, tsr^{UAS}]2/w, P[ry^+; GMR(Gal4-Pc)]1 tsr^{N96A}/tsr^{N96A}; (H) *y w* P[w^+, tsr^{UAS}]2/w, P[ry^+; GMR(Gal4-Pc)]2 tsr^{N96A}/tsr^{N96A}.
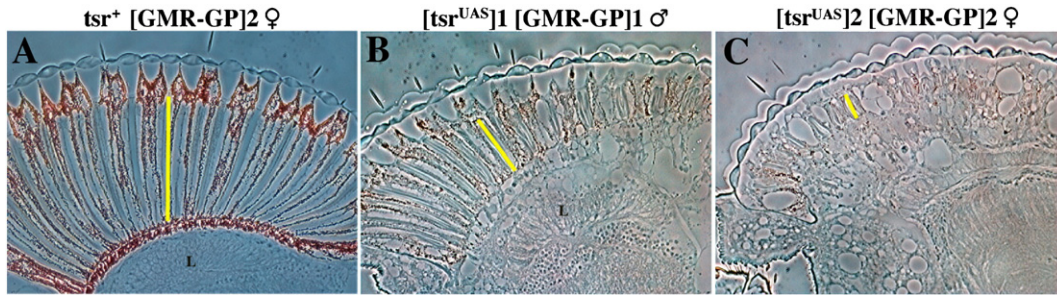
Fig. 3. Longitudinal sections show that *tsr* RS mutants have thin retinas. One day old flies were fixed and cross-sectioned to determine the length of the retina. (A) Female flies having the construct GMR(Gal4-Pc) express Gal4-Pc in the eye but do not have a mutant phenotype because they have a wild type *tsr*[+] allele. Weak (B) and strong (C) *tsr* RS mutants were found to have a thin retina when compared to the control. The yellow line shows the thickness of the retina. A lamina (L) is not found in the strongest mutant (C). Genotypes for the flies are (A) *w*, P[*ry*[+]; GMR(Gal4-Pc)]2 *tsr*[N96A]/CyO female; (B) *y w* P[*w*[+], *tsr*[UAS]]1/Y, P[*ry*[+]; GMR(Gal4-Pc)]1 *tsr*[N96A]/*tsr*[N96A] male; (C) *y w* P[*w*[+], *tsr*[UAS]]2/*w*, P[*ry*[+]; GMR(Gal4-Pc)]2 *tsr*[N96A]/*tsr*[N96A] female. Anterior is on the left, posterior on the right.

and Steller, 1991), suggesting that there may be an innervation defect in the stronger mutants.

twinstar RS mutations alter the actin cytoskeleton in pupal eye discs

Eye imaginal discs of the *tsr* RS mutants were analyzed at various time points to identify the stage that the defects were first seen. The GMR promoter in P[*ry*[+]; *GMR*(*Gal4-Pc*)] initiates expression of Gal4-Pc in the 3rd instar larval eye disc; however, no defect was detected at that stage (data not shown). This lack of a 3rd instar larval phenotype is likely explained by a lag in the RS system. The GMR promoter will initiate transcription in cells positioned at or behind the morphogenetic furrow (Moses and Rubin, 1991), resulting in the transcription and translation of Gal4-Pc in these cells. Only when a sufficient concentration of Gal4-Pc is made can it bind to the UAS sites in *tsr*[UAS] and repress transcription. At that time the concentration of the *tsr* mRNA will start to decrease, followed by a reduction in the concentration of Tsr protein, the rate of decrease dependent on the half-life of both mRNA and protein. The concentration of Tsr protein will eventually decrease to a level low enough to impair development. The data suggest that this lag persists throughout larval development. When 60-h APF (after pupal formation) eye discs were analyzed, a mutant phenotype was found. There were clear differences between the F-actin distributions in wild type and *tsr* RS mutants. In apical sections, there was a significant increase in F-actin in the two primary pigment cells of each ommatidium (Figs. 4D, G), and an increase in F-actin concentration was also seen in basal cross-sections of the *tsr* RS mutants (Figs. 4F, I). An increase in the concentration of F-actin was
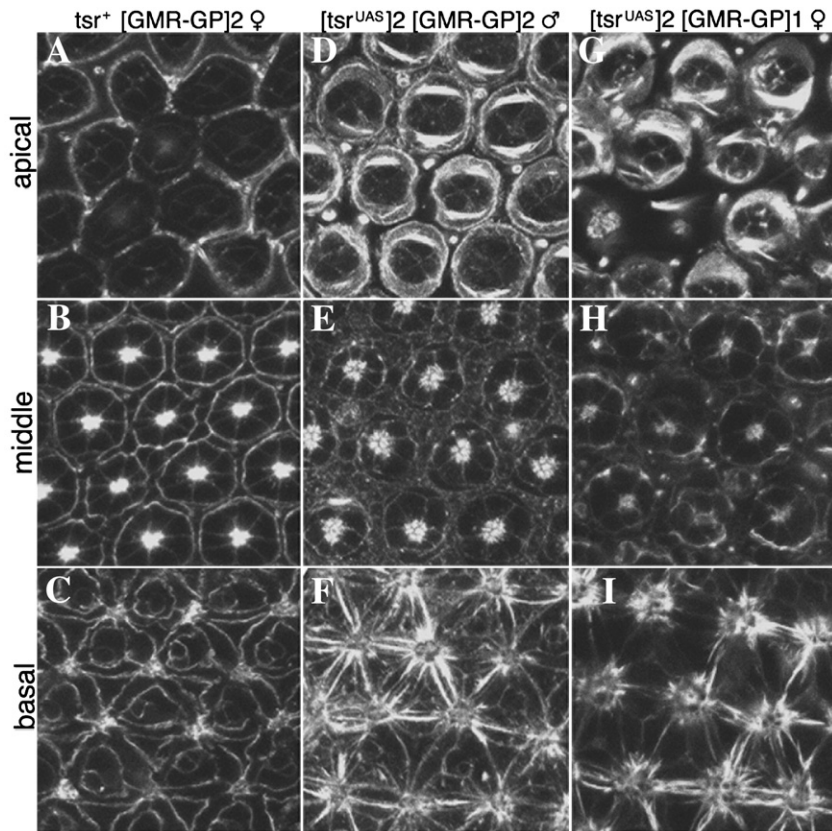

Fig. 4. *tsr* RS mutants have a pupal eye defect. Pupae were dissected 60 h after pupal formation at 25 °C (60% of pupal development) and stained with rhodamine-conjugated phalloidin. A–C show apical, middle, and basal confocal cross-sections of the control, a P[*ry*[+]; GMR(Gal4-Pc)]2/CyO female. D–F are of an intermediate *tsr* RS mutant of the genotype *y w* P[*w*[+], *tsr*[UAS]]2/Y, P[*ry*[+]; GMR(Gal4-Pc)]2 *tsr*[N96A]/*tsr*[N96A] male and G–I are of a strong *tsr* RS mutant of the genotype *y w* P[*w*[+], *tsr*[UAS]]2/*w*, P[*ry*[+]; GMR(Gal4-Pc)]1 *tsr*[N96A]/*tsr*[N96A] female.

expected in a *tsr* loss of function mutant due to the decrease in F-actin depolymerizing activity, and was observed previously in *tsr* mutant ovaries (Chen et al., 2001). In the control, the rhabdomeres expressed high levels of F-actin (Fig. 4B). The intensity of F-actin staining was the same in the intermediate mutant; however, the rhabdomeres were not as compact (Fig. 4E). Surprisingly, there were decreases in the intensity of F-actin staining in the rhabdomeres of the strong *tsr* RS mutant, suggesting a direct *tsr* requirement during rhabdomere morphogenesis (Fig. 4H). Examination shows that all the expected cell types were present in the *tsr* RS mutants (data not shown). This indicates that cell division and differentiation occurred normally in the mutant, and therefore the *tsr* RS mutant phenotypes were the result of a defect in morphogenesis.

twinstar RS mutations cause rhabdomere defects

The rhabdomere structures of *tsr* RS mutants were analyzed by transmission electron microscopy (TEM). A wild type eye had an ordered array of ommatidia with seven rhabdomeres detected in each section of an ommatidium (Figs. 5A, B). Higher magnification shows that each rhabdomere is composed of many microvilli, each a finger-like extension of the membrane, providing an enlarged surface for rhodopsin (Fig. 5C). Consistent with the F-actin staining pattern, the rhabdomeres of a strong *tsr* RS mutant were smaller than normal, and had a disorganized structure and microvilli of variable length (Figs. 5G–I). The integrity of the rhabdomere was frequently not maintained allowing microvilli to "unravel" (Fig. 5I, arrow). These data suggest a role for *tsr* during the morphogenesis of the rhabdomere microvilli. These defects were less severe in the intermediate mutant, where the length of the individual microvilli was only slightly shorter than normal and does not unravel (Figs. 5D–F). However, the rhabdomeres of the intermediate mutants were abnormal in shape, either wider than normal or split in two. We believe these two shapes were related, that widened rhabdomeres were unstable and sometimes folded in half. These widened rhabdomeres result in an increased size of the rhabdomeres in a section through the ommatidia. For instance, the total area of the seven rhabdomeres shown in the intermediate tsrRS mutant (panel 5E) is 1.8-fold larger than the area of the seven rhabdomeres shown in the control (panel 5B). However, since the tsrRS mutant retina is significantly thinner than the control, the total volume of rhabdomere is not increased in the mutant cell. In addition to widened rhabdomeres, the adherens junctions of many of the mutant photoreceptor cells were also elongated (compare arrowheads in Figs. 5C and F). Another phenotype is that the ommatidia are not as densely packed in the mutant as in the control (compare Figs. 5A and D). Sections were taken from the middle of each retina. During retinal elongation, the ommatidia acquire a tapered shape, with the basal footprint being appreciably smaller than the apical headprint. We believe that the observed difference in density is the result of the *tsr* RS mutants not tapering because of the lack of retinal elongation.

Relationship between the lack of retinal cell elongation and the widening of rhabdomeres and adherens junctions

The intermediate strength *tsr* RS mutation had three distinct mutant phenotypes: (1) a lack of retinal cell elongation; (2) widened rhabdomeres; and (3) widened adherens junctions. Cofilin/ADF likely has many functions during retinal morphogenesis, it is therefore possible that it directly regulates these characteristics, resulting in the observed defects. However, it is also possible that these phenotypes are not independent. We propose that *tsr* is directly required for the reorganization of the actin cytoskeleton during retinal elongation. But
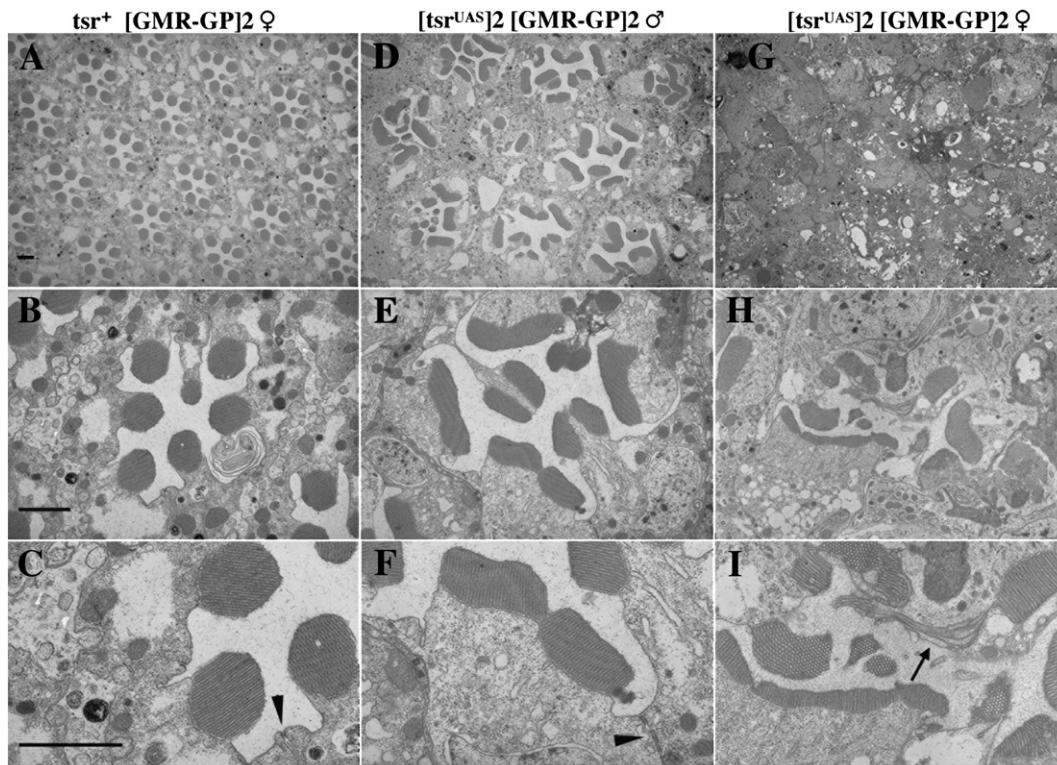

Fig. 5. *tsr* RS mutants have rhabdomere and adherens junctions defects. (A–C) The control P[*ry*+; GMR(Gal4-Pc)]2/CyO female fly was fixed, sectioned, and photographed at different magnifications by TEM. (D–F) The intermediate *tsr* RS mutant has a lower density of ommatidia than the control. Many rhabdomeres are wider than normal or split. The adherens junctions of *tsr* RS mutants are frequently also wider than the control (compare arrowheads in C and F). (G–I) Ommatidial structures are difficult to see at low magnification in the strong *tsr* RS mutant. At higher magnification, the rhabdomeres are highly irregular in structure. Unraveled microvilli are frequently seen in the strong mutant (arrow in I). A, D, and G were taken at 1900× magnification and B, E, and H at 7200×. C, F, and I are two-fold blowups of B, E, and H. Scale bars are all 2 μM.

how to explain the widened rhabdomeres and adherens junctions? As the retinal cells elongate five-fold in the visual axis, the rhabdomeres and adherens junctions also elongate along that axis (Fig. 1A). There must be high levels of expression of rhabdomere and adherens junction proteins to allow this growth to occur. We propose that in a mutant in which elongation does not occur, there is little or no feedback control telling the cell not to make the extra rhabdomere and adherens junction proteins. If so, these proteins will still be made at high levels and will likely still be transported to the rhabdomeres and adherens junctions. However, since the rhabdomeres and adherens junctions are not elongating along the visual axis, we propose they widen, causing the observed phenotypes.

As a first test of this hypothesis, we asked at what stage of development do the rhabdomeres and adherens junctions undergo their abnormal widening in a tsr RS mutant. The rhabdomeres begin to form at about 35% of pupal development, and the five-fold retinal elongation starts slightly before 55% of pupal development and continues through eclosion. If the hypothesis is correct, the size of the rhabdomeres and adherens junctions will be normal at the time retinal elongation should begin, and widens only at later stages after elongation should have occurred. TEM analysis was therefore done on tsr RS mutant eye discs at 55% and 73% of pupal development. Fig. 6 shows that the tsr RS rhabdomeres were of approximately normal size at 55% of pupal development (compare Fig. 6B with A), but the tsr RS rhabdomeres were significantly wider than wild type at 73% of pupal development (compare Fig. 6D with C). Another way to look at it, the width of the rhabdomeres stayed approximately the same during wild type development (Figs. 6A, C) but increased significantly in the tsr RS mutant (Figs. 6B, D). The large increase in rhabdomere width is therefore only detected in the tsr RS mutant after retinal elongation should have occurred, consistent with the above hypothesis. Similar results were seen with the adherens junction phenotype. At 55% of

pupal development, the sizes of the adherens junctions were similar in control and mutant (Figs. 6A, B), but by 73% of pupal development, the control was significantly smaller than the mutant adherens junction (Figs. 6C, D). Interestingly, this appears to be primarily caused by a decrease in the size of the control (Figs. 6A, C), rather than an increase in the size of the adherens junction in the tsr RS mutant (Figs. 6B, D).

Cytoskeletal genes have retinal mutant phenotypes similar to tsr

To determine whether the phenotypes observed in the tsr RS mutants were specific to tsr, or whether they were indicative of a general defect in actin reorganization, we asked whether similar phenotypes are seen in mutants of other actin cytoskeletal proteins. Slingshot protein is a phosphatase that cleaves phosphate from Tsr, activating it. Using somatic mosaic analysis, eyes containing ssh mosaic clones had rough eyes and ommatidia with a reduced number of photoreceptor cells (Fig. 7A). In addition, many cells had widened or split rhabdomeres, similar to the tsr RS mutants. Widened rhabdomeres were also seen in mosaic clones of capping protein beta (Fig. 7B) and Arc-p34, a member of the Arp2/3 complex (Fig. 7C). As with tsr, we believe these widened rhabdomeres were the result of a lack of retinal elongation. This was demonstrated in the Arc-p34 mutant by serial sectioning, showing that some of the mutant cells with widened rhabdomeres do not extend the entire length of the retina (arrow in Fig. 7C).

The tsr RS mutation genetically interacts with mutations in tsr regulatory genes

The tsr RS mutations are dosage sensitive, as demonstrated by the stronger phenotype in female flies. We asked whether the tsr RS
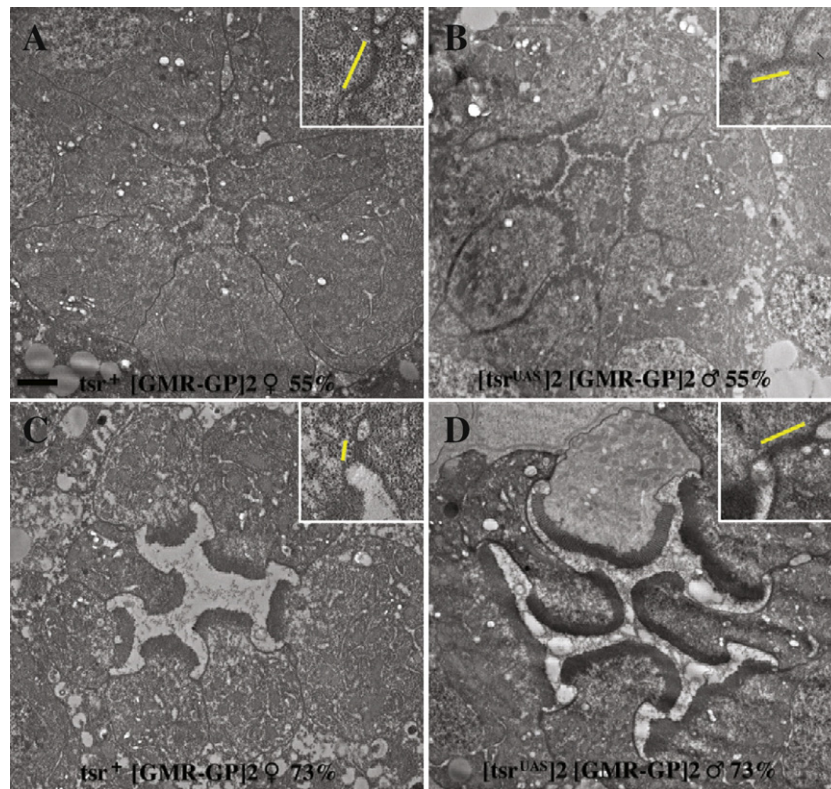

Fig. 6. The widening of tsr RS mutant rhabdomeres and adherens junctions takes place late in pupal development. (A, C) The control P[ry+; GMR(Gal4-Pc)]2/CyO female and (B, D) an intermediate strength tsr RS P[w+; tsr^UAS]2 P[ry+; GMR(Gal4-Pc)]2 tsr^Δ96 male were analyzed by TEM at 55% (A, B) and 73% (C, D) of pupal development. At 55% pupal development, the rhabdomere and adherens junction of the control and tsr RS mutant are appropriately equal. At 73% pupal development, the rhabdomeres and adherens junction of the tsr RS mutant is significantly wider than the control (C). Inset within each panel is a two-fold blowup of an adherens junction, with the yellow line displaying its size. Scale bar is 1 μM.
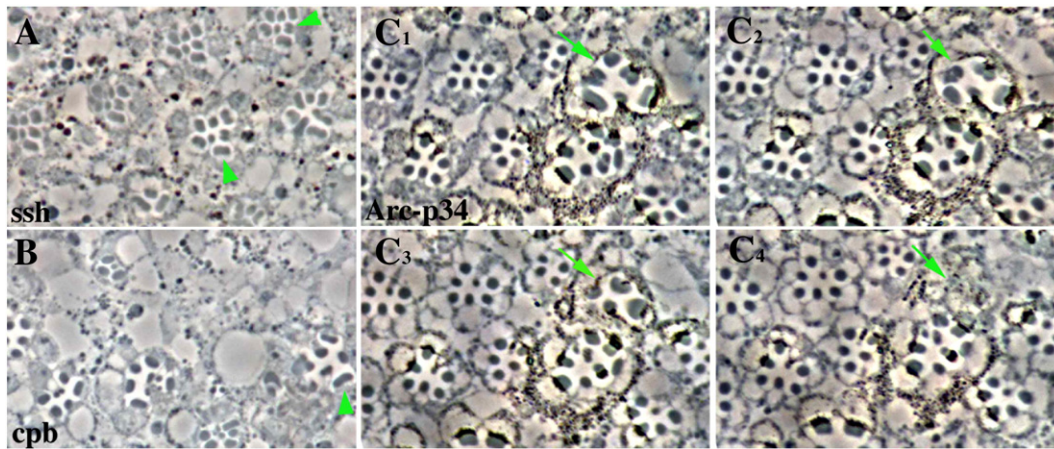
Fig. 7. Widened rhabdomeres are found in photoreceptor cells mutant for genes that are involved in the reorganization of the actin cytoskeleton. The FLP/FRT system was used to make somatic mosaics of the mutant alleles of (A) ssh^{1-11}, (B) cpb^{M143}, and (C1–C4) $Arc-p34^{KG04658}$. The mosaic eyes were fixed and sectioned. (A, B) Examples of widened or split rhabdomeres are indicated by arrowheads. C1–C4 contain a series of four adjacent serial sections. The arrow points to an ommatidia containing photoreceptors with widened rhabdomeres. These rhabdomeres do not extend the full length of the retina and terminate within the serial sections shown. The $Arc-p34^{KG04658}$ allele is marked with a mini-*white* gene. Heterozygous cells have low levels of pigment, with the homozygous mutant cells being more darkly pigmented.

phenotype can be modified by mutations in genes thought to be able to interact with *tsr*, and found that mutations in both *ssh* (Niwa et al., 2002; Rogers et al., 2005) and *flare* (the *Drosophila* homologue of Aip1; Ren et al., 2007) were able to enhance the *tsr* RS mutant phenotype. Actin interacting protein 1 (Aip1) works with cofilin/ADF to promote actin depolymerization (Okada et al., 1999). Using a strong *tsr* RS mutant, the number and size of black necrotic spots on the eye increased if the *tsr* RS mutant fly were heterozygous for a mutation in *ssh* (Fig. 8B) or *flare* (Fig. 8D). Also, heterozygosity in *ssh* or *flare* can elicit abnormal rhabdomere structures in a weak *tsr* RS mutant background (Figs. 8E–H).

Discussion

Analysis of *tsr* RS mutations suggests that *tsr* has an important role in retinal cell elongation and in the morphogenesis of the rhabdomere. During wild type development, retinal cells undergo five-fold elongation, whereas this elongation is defective in *tsr* RS mutants.
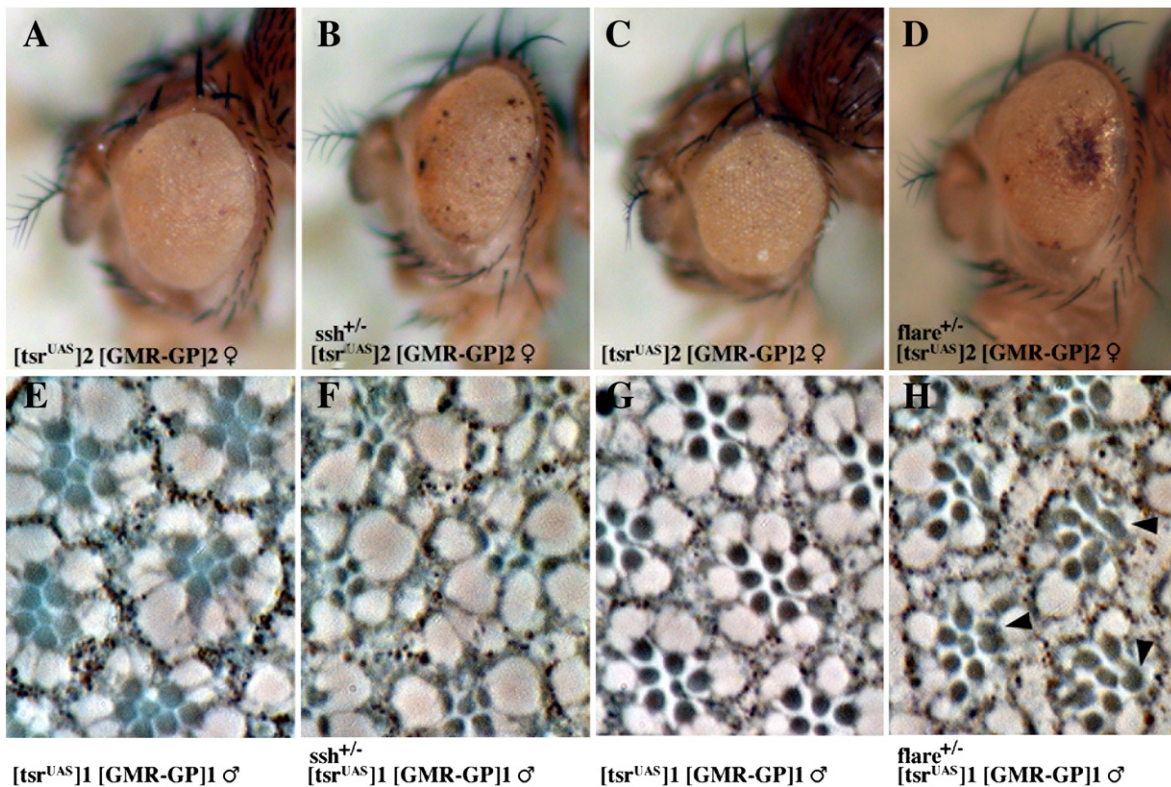

Fig. 8. Mutations in *ssh* and *flare* enhance the *tsr* RS mutant phenotypes. (A–D) The P[w⁺; tsr^UAS]2 P[ry⁺; GMR(Gal4-Pc)]2 female *tsr* RS mutant eye phenotype is enhanced and shows a higher rate of necrosis if the fly is heterozygous for (B) ssh^{26-1} or (D) $flare^{BG2697R\#5}$. Sections through *tsr* RS eyes show that *ssh* and *flare* can also enhance a *tsr* RS rhabdomere mutant phenotype. For this analysis, the phenotype of the weak *tsr* RS mutant P[w⁺; tsr^UAS]1 P[ry⁺; GMR(Gal4-Pc)]1 males (E–H) was enhanced by heterozygous mutations in (F) ssh^{26-1}, where the rhabdomere morphology and organization are more disrupted, and (H) $flare^{BG2697R\#5}$, where some rhabdomeres are split or have abnormal shapes (arrowheads).

Strong *tsr* mutants also showed additional defects in rhabdomere morphogenesis, as noted by a severe reduction in F-actin in the pupal rhabdomere, and by rhabdomere defects displayed by TEM analysis. These defects included shortened microvilli, suggesting a *tsr* role in microvilli morphogenesis. In addition, in many instances, a microvilli or set of microvilli appeared to "unravel" from the rhabdomere, indicating a role for *tsr* in maintenance of the rhabdomere structure. It had been hypothesized that the actin rich rhabdomere terminal web is required to maintain the organization of the microvilli (Ready, 2002). The observed phenotype is consistent with *tsr* functioning as part of the rhabdomere terminal web to stabilize the rhabdomere structure.

Rhabdomeres in intermediate *tsr* RS mutants were wider than normal. While it is possible that *tsr* is directly involved in shaping the rhabdomere, we presented a second possibility, that the widened rhabdomeres are a secondary event caused by the lack of retinal elongation. This hypothesis suggests that there is incomplete feedback in the *tsr* RS mutant, preventing the cell from recognizing that it is not elongating. The *tsr* RS mutant photoreceptor cells therefore produce all the rhabdomere proteins necessary for a fully elongated cell, but when the mutant cell does not elongate, a short but wide rhabdomere forms. However, the relationship between length and width is not fluid, there is not a one to one correlation between a lack of rhabdomere elongation and an increased in width. For instance, in the weakest tsrRS mutant, retinal elongation is inhibited by about 50% (Fig. 3B), yet rhabdomeres from this weak mutant are wild type in width (data not shown). We therefore believe that there are cellular mechanisms that maintain that correct size and shape of the rhabdomere, and only when this mechanism is stressed beyond a certain threshold (such as in the intermediate mutant) do the widened rhabdomeres appear. As predicted by the hypothesis, the widened rhabdomeres only formed in the *tsr* RS mutant after retinal elongation should have begun. Widened adherens junctions were also observed in the *tsr* mutant, this is likely also due to a lack of retinal elongation. Interestingly, we found that the retinal adherens junctions in a wild type 55% pupae are wider than in a wild type 73% pupae. It is therefore likely that the cell builds up adherens junction proteins in anticipation of retinal elongation, then during elongation these excess proteins converge and extend to form the longer but slimmer adult adherens junction. Many adherens junctions in the 73% pupal *tsr* mutant were wider than wild type, suggesting that inhibition of retinal elongation prevents this conversion and extension from occurring.

Black patches of necrotic cells are frequently observed in the strong *tsr* RS mutants. It is possible that this necrotic phenotype is a secondary effect due to a lack of retinal cell elongation. As the retinal cells elongate, they increase in volume. However, if the cytoskeleton cannot change its structure as the cell increases in volume, and there is no feedback telling the cell this, the result may be that the cell overgrows its support structure and bursts, committing necrosis.

Many *Drosophila* mutants have widened rhabdomeres as a mutant phenotype. Our data suggest the possibility that these widened rhabdomeres are secondary effects due to a blockage of retinal elongation. For example, photoreceptor cells mutant for *crumbs*, a transmembrane apical determinant, have a complicated phenotype, but the mutant cells are shorter than wild type and also have widened rhabdomeres and adherens junctions (Izaddoost et al., 2002; Pellikka et al., 2002). Our results suggest that these *crumbs* mutant phenotypes may be related, that *crumbs* may be directly required for retinal elongation, and, as with *tsr*, that the rhabdomere and adherens junction phenotypes may be secondary events.

The above hypothesis provides an explanation for the widened rhabdomeres and adherens junctions, but does not explain why *tsr* is required for retinal elongation. As a first step to addressing this, we found that mutations in three other cytoskeletal genes (*ssh*, *capping protein* β and *Arc-p34*) had wide rhabdomeres, suggesting an inhibition of retinal elongation, which was verified by serial section analysis of the *Arc-p34* mutant. This indicates that the defect in retinal elongation is not a *tsr* specific mutant phenotype, but is instead a general mutant phenotype for the inability to reorganize the actin cytoskeleton during retinal elongation.

This study introduces a new kind of conditional lethal mutation that we call a repressor sensitive mutation. The main advantage of this technique is its tissue specificity, it can reduce gene activity specifically in one tissue by driving Gal4-Pc from a tissue specific promoter. This technique should be adaptable to any gene in which a genomic rescue construct is available. Theoretically, this technique should also be able to repress the expression of endogenous genes that are adjacent to a P element insertion containing UAS sites. An unexpected advantage of the repressor sensitive technique was the easily established phenotypic series. A combination of position effect and dosage compensation provided a series of mutants whose phenotypes varied from weak, to intermediate to strong. This series allowed us to characterize microvilli formation in the strong mutant, and retinal elongation and the widening of the rhabdomeres and adherens junctions in the intermediate mutant. In addition, we are currently using the weak *tsr* RS mutations to study the role of *tsr* during phototransduction (Hung Pham, personal communication). The further development of the repressor sensitive technique will add to the already large group of genetic tools available to *Drosophila* researchers.

Experimental procedures

DNA constructs

To make P[w^+;tsr^{UAS}], the complementary oligonucleotides 5′ AATTCGGCCGCTGCAGAAATCTAGACGGCCGA and 5′AGCTTCGGCCGTC-TAGATTTCTGCAGCGGCCG were cloned into the *Eag*I site located 43 bp downstream from the 5′ end of the first intron of *tsr* in P[mini-w^+; tsr^+], which contains the *tsr* 6.4 kb genomic rescue construct (Gunsalus et al., 1995). The oligos contain internal *Pst*I and *Xba*I restriction enzyme sites, into which was cloned a small *Pst*I–*Xba*I fragment of G$_5$E4T (Lin et al., 1988) that contains 5 copies of the Gal4 17-mer (Giniger et al., 1985). Transformation into y w^{67} flies used standard techniques.

P[ry^+; GMR(Gal4-Pc)] was made by subcloning the *Xho*I–*Eco*RI fragment of the pGMR promoter (from −265 to +210) into Bluescript. The *Xho*I and *Eco*RI sites were then modified so that they could be inserted into the *Not*I and *Xba*I sites that are located between the hsp70 sequences and the Gal4 sequences of hs(Gal4-Pc) (Muller, 1995). Transformation into ry^{506} flies used standard techniques.

Fly lines and genetic crosses

For the genetic interactions studies between *tsr* and *ssh*; w, P[ry^+; GMR(Gal4-Pc)]2 $tsr^{Δ96}$/CyO, ssh^{26-1}/MKRS Sb males were crossed to y w P[w^+;tsr^{UAS}]2, $tsr^{Δ96}$ females and w, P[ry^+; GMR(Gal4-Pc)]1 $tsr^{Δ96}$/CyO, ssh^{26-1}/MKRS Sb males were crossed to y w P[w^+;tsr^{UAS}]1, $tsr^{Δ96}$ females. ssh^{26-1} is a P-element insertion mutation into *ssh* locus (Niwa et al., 2002). For the genetic interactions studies between *tsr* and *flare*; w, P[ry^+; GMR(Gal4-Pc)]2 $tsr^{Δ96}$/CyO, $aip1^{BG2697R5}$/MKRS Sb males were crossed to y w P[w^+;tsr^{UAS}]2, $tsr^{Δ96}$ females and w, P[ry^+; GMR (Gal4-Pc)]2 $tsr^{Δ96}$/CyO, $flare^{BG2697R5}$/MKRS Sb males were crossed to y w P[w^+;tsr^{UAS}]2, $tsr^{Δ96}$ females. $flare^{BG2697R5}$ is a strong allele of *aip1* that was generated by imprecise excision of the P element in the $flare^{BG2697}$ allele (Chen and Laski, unpublished data). MKRS is a 3rd chromosome balancer having the genotype Tp(3;3)MRS M(3)76A^1 Sb^1 kar^1 ry^2.

Mosaic analysis

The loss-of-function allele cpb^{M143} was recombined to an FRT component on 2L chromosome as described (Chen et al., 2005). Flies

containing homozygous somatic mosaic clones in eyes were generated using the FLP/FRT system (Xu and Rubin, 1993). y^1 w^*; P [neoFRT]82B ssh$^{1-11}$/TM3, y^+ Ser^1 flies were crossed to y^{d2} w^{1118} P[ey-FLP.N]2 P[GMR-lacZ.C(38.1)]TPN1, P[neoFRT]82B, while y^{d2} w^{1118} P [ey-FLP.N]2 P[GMR-lacZ.C(38.1)]TPN1, cpb^{M143} P[neoFRT]40A/CyO and y^{d2} w^{1118} P[ey-FLP.N]2 P[GMR-lacZ.C(38.1)]TPN1, P[SUPor-P] Arc-p34^{KG04658} P[neoFRT]40A/CyO y^+ were crossed to y^{d2} w^{1118} P [ey-FLP.N]2 P[GMR-lacZ.C(38.1)]TPN1, P[neoFRT]40A.

The stock y^1 w^*; P[neoFRT]82B ssh$^{1-11}$/TM3, y^+ Ser^1 was obtained from Kevin Moses lab. The stock cpb^{M143} cn^1 b^1 sp^1/CyO was obtained from the Bloomington stock center. Stocks y^{d2} w^{1118} P[ey-FLP.N]2 P [GMR-lacZ.C(38.1)]TPN1, P[SUPor-P]Arc-p34^{KG04658} P[neoFRT]40A/ CyO y^+, and y^{d2} w^{1118} P[ey-FLP.N]2 P[GMR-lacZ.C(38.1)]TPN1, P [neoFRT]40A, and y^{d2} w^{1118} P[ey-FLP.N]2 P[GMR-lacZ.C(38.1)]TPN1, P [neoFRT]82B were obtained from UCLA undergraduate research consortium in Functional Genomics.

Collecting and aging pupae

Pupae were aged according to Kumar and Ready (1995). Late third instar larvae (grown at 25 °C) were isolated and males and females separated. They were then grown overnight at 18 °C on yeasted vials. Next morning, the white pre-pupae were collected and grown at 20 °C. Pupal development at 20 °C is 172 h. Pupae at 55% of development were harvested 95 h later, 73% of development 126 h later.

Histological analysis

The protocol for preparing pupal eyes for TEM analysis was adapted from Kumar and Ready (1995). Day 1: Pupal eye discs were dissected in phosphate buffer (0.1 M, pH 7.4) and quickly transferred to fix solution (0.875% glutaraldehyde, 1% formaldehyde, and 0.025 M sodium cacodylate) for 1 h on ice, transferred to a fresh fix solution for 4 h on ice, then incubated overnight in fresh fix solution with 1% tannic acid. Day 2: Discs were washed 3 times for 10 min in phosphate buffer, then incubated 2 times for 10 min in 0.1 M sodium cacodylate, followed by a 2 h incubation in 4% osmium tetroxide. The discs were washed 3× with double distilled H_2O and incubated in 2% uranyl acetate overnight. Day 3: Discs were washed 2 times for 10 min in dd H_2O, dehydrated in 50%, 70%, 85%, and 95% EtOH for 5 min each at room temperature, then 100% EtOH 2 times for 10 min at room temperature. This was followed with dehydration with propylene oxide (2 times for 7 min at room temperature) and incubated with a propylene oxide: Durcupan plastic (1:1) mixture overnight at room temperature. Day 4: Eye discs were imbedded in Durcupan plastic and incubated overnight at 60 °C.

The protocol for preparing adult eyes for TEM analysis was adapted from Pellikka et al. (2002). Fly heads were severed and bisected in phosphate buffer. The eye (bisected head) was quickly transferred to a fixing solution (2.5% glutaraldehyde, 2% formaldehyde, 0.1 M sodium cacodylate, pH 7.4) on ice in an Eppendorf tube, then fixed for 3 days at 4 °C in a rotator. Eyes were then washed 3 times for 10 min in phosphate buffer on ice, then incubated in 1% osmium tetroxide in 0.1 M sodium cacodylate (pH 7.4) and 0.1 M sorbitol for 1 h at room temperature. Eyes were then washed 2 times with phosphate buffer for 10 min each at room temperature, followed by dehydration in 50%, 70%, 85%, and 95% EtOH for 5 min each at room temperature, followed by 2 washes (10 min each) in 100% EtOH at room temperature. This was followed with dehydration with propylene oxide (2 times for 7 min at room temperature) and incubated with a propylene oxide: Durcupan plastic (1:1) mixture overnight at room temperature. The eyes were then imbedded in Durcupan plastic and incubated overnight at 60 °C.

Seventy nanometer thin sections were obtained using a Leica EM UC6 Microtome. The sections were picked up on an EM grid and dried at room temperature. The grids were then floated section side down on a uranyl acetate solution (1/3 saturated uranyl acetate, 1/3 100% EtOH, and 1/3 water) for 30 min at room temperature, then quickly washed 3 times in dd H_2O, and transferred grid side down onto a lead citrate solution for 3 min. The lead citrate solution was made by adding 30 ml of air free dH_2O (by boiling dH_2O to get rid of CO_2) plus 1.33 g lead citrate, 1.76 g sodium citrate, and 8 ml of 1 N NaOH. This was followed by washing 3 times in dd H_2O, with blotting of the excess water from the grid.

Pupal dissection and phalloidin staining protocols were modified from *Drosophila Protocols* (Sullivan et al., 2000).

Microscopy

TEM images were obtained by using a Hitachi TEM H-7000 microscope (UCLA MBI Electron Microscopy Facility) or a Jeol JEM-100CX II Electron Microscope (UCLA EM Core Facility). The relative size of the rhabdomeres in the tsrRS mutant and control was determined using Adobe Photoshop software. Confocal microscopy was done at the CNSI Advanced Light Microscopy/Spectroscopy Shared Facility using Leica Confocal Software (Leica Microsystems, Heidelberg GmbH). Scanning electron microscopy images were obtained by using Hitachi S-2460N and Quartz PCI Version 3 imaging system software.

Appendix A. Supplementary data

Supplementary data associated with this article can be found, in the online version, at doi:10.1016/j.ydbio.2008.03.006.

References

Arber, S., Barbayannis, F.A., Hanser, H., Schneider, C., Stanyon, C.A., Bernard, O., Caroni, P., 1998. Regulation of actin dynamics through phosphorylation of cofilin by LIM-kinase. Nature 393, 805–809.

Bamburg, J.R., McGough, A., Ono, S., 1999. Putting a new twist on actin: ADF/cofilins modulate actin dynamics. 9, 364–370.

Bi, E., Zigmond, S.H., 1999. Actin polymerization: where the WASP stings. Curr. Biol. 9, R160–R163.

Blanchoin, L., Amann, K.J., Higgs, H.N., Marchand, J.-B., Kaiser, D.A., Pollard, T.D., 2000. Direct observation of dendritic actin filament networks nucleated by Arp2/3 complex and WASP/Scar proteins. Nature 404, 1007–1110.

Cagan, R.L., Ready, D.F., 1989. The emergence of order in the *Drosophila* pupal retina. Dev. Biol. 136, 346–362.

Carlier, M.-F., 1998. Control of actin dynamics. Curr. Opin. Cell Biol. 10, 45–51.

Carlier, M.F., Pantaloni, D., 1997. Control of actin dynamics in cell motility. J. Mol. Biol. 269, 459–467.

Chen, J., Godt, D., Gunsalus, K., Kiss, I., Goldberg, M., Laski, F.A., 2001. Cofilin/ADF is required for cell motility during *Drosophila* ovary development and oogenesis. Nat. Cell Biol. 3, 204–209.

Chen, J., Call, G.B., Beyer, E., Bui, C., Cespedes, A., Chan, A., Chan, J., Chan, S., Chhabra, A., Dang, P., Deravanesian, A., Hermogeno, B., Jen, J., Kim, E., Lee, E., Lewis, G., Marshall, J., Regalia, K., Shadpour, F., Shemmassian, A., Spivey, K., Wells, M., Wu, J., Yamauchi, Y., Yavari, A., Abrams, A., Abramson, A., Amado, L., Anderson, J., Bashour, K., Bibikova, E., Bookatz, A., Brewer, S., Buu, N., Calvillo, S., Cao, J., Chang, A., Chang, D., Chang, Y., Chen, Y., Choi, J., Chou, J., Datta, S., Davarifar, A., Desai, P., Fabrikant, J., Farnad, S., Fu,

K., Garcia, E., Garrone, N., Gasparyan, S., Gayda, P., Goffstein, C., Gonzalez, C., Guirguis, M., Hassid, R., Hong, A., Hong, J., Hovestreydt, L., Hu, C., Jamshidian, F., Kahen, K., Kao, L., Kelley, M., Kho, T., Kim, S., Kim, Y., Kirkpatrick, B., Kohan, E., Kwak, R., Langenbacher, A., Laxamana, S., Lee, C., Lee, J., Lee, S.Y., Lee, T.H., Lee, T., Lezcano, S., Lin, H., Lin, P., Luu, J., Luu, T., Marrs, W., Marsh, E., Min, S., Minasian, T., Misra, A., Morimoto, M., Moshfegh, Y., Murray, J., Nguyen, C., Nguyen, K., Nodado II, E., O'Donahue, A., Onugha, N., Orjiakor, N., Padhiar, B., Pavel-Dinu, M., Pavlenko, A., Paz, E., et al., 2005. Discovery-based science education: functional genomic dissection in *Drosophila* by undergraduate researchers. PLoS Biol. 3, e59.

Ellis, M.C., O'Neill, E.M., Rubin, G.M., 1993. Expression of *Drosophila* glass protein and evidence for negative regulation of its activity in non-neuronal cells by another DNA-binding protein. Development 119, 855–865.

Giniger, E., Varnum, S.M., Ptashne, M., 1985. Specific DNA binding of GAL4, a positive regulatory protein of yeast. Cell 40, 767–774.

Gunsalus, K.C., Bonaccorsi, S., Williams, E., Verni, F., Gatti, M., Golberg, M., 1995. Mutations in twinstar, a *Drosophila* gene encoding a cofilin/ADF homologue, result in defects in centrosome migration and cytokinesis. J. Cell Biol. 131, 1243–1259.

Higgs, H.N., Pollard, T.D., 1999. Regulation of actin polymerization by Arp2/3 complex and WASp/Scar proteins. J. Biol. Chem. 274, 32531–32534.

Izaddoost, S., Nam, S.C., Bhat, M.A., Bellen, H.J., Choi, K.W., 2002. *Drosophila* Crumbs is a positional cue in photoreceptor adherens junctions and rhabdomeres. Nature 416, 178–183.

Kumar, J.P., Ready, D.F., 1995. Rhodopsin plays an essential structural role in *Drosophila* photoreceptor development. Development 121, 4359–4370.

Kunes, S., Steller, H., 1991. Ablation of *Drosophila* photoreceptor cells by conditional expression of a toxin gene. Genes Dev. 5, 970–983.

Lin, Y.S., Carey, M.F., Ptashne, M., Green, M.R., 1988. GAL4 derivatives function alone and synergistically with mammalian activators in vitro. Cell 54, 659–664.

Longley Jr., R.L., Ready, D.F., 1995. Integrins and the development of three-dimensional structure in the *Drosophila* compound eye. Dev. Biol. 171, 415–433.

Machesky, L.M., Cooper, J.A., 1999. Bare bones of the cytoskeleton. Nature 401, 542–543.

Maskery, S., Shinbrot, T., 2005. Deterministic and stochastic elements of axonal guidance. Annu. Rev. Biomed. Eng. 7, 187–221.

McGough, A., Pope, B., Chiu, W., Weeds, A., 1997. Cofilin changes the twist of F-actin: implications for actin filament dynamics and cellular function. J. Cell Biol. 138, 771–781.

Moses, K.E., 2002. *Drosophila* eye development. Results and Problems in Cell Differentiation, vol. 37, p. 282.

Moses, K., Rubin, G.M., 1991. Glass encodes a site-specific DNA-binding protein that is regulated in response to positional signals in the developing *Drosophila* eye. Genes Dev. 5, 583–593.

Muller, J., 1995. Transcriptional silencing by the Polycomb protein in *Drosophila* embryos. EMBO J. 14, 1209–1220.

Niwa, R., Nagata-Ohashi, K., Takeichi, M., Mizuno, K., Uemura, T., 2002. Control of actin reorganization by Slingshot, a family of phosphatases that dephosphorylate ADF/cofilin. Cell 108, 233–246.

Okada, K., Obinata, T., Abe, H., 1999. XAIP: a *Xenopus* homologue of yeast actin interacting protein 1 (AIP1), which induces disassembly of actin filaments cooperatively with ADF/cofilin family proteins. J. Cell Sci. 112, 1553–1565.

Pantaloni, D., Le_Clainche, C., Carlier, M.F., 2001. Mechanism of actin-based motility. Science 292, 1502–1506.

Pellikka, M., Tanentzapf, G., Pinto, M., Smith, C., McGlade, C.J., Ready, D.F., Tepass, U., 2002. Crumbs, the *Drosophila* homologue of human CRB1/RP12, is essential for photoreceptor morphogenesis. Nature 416, 143–149.

Pollard, T.D., Borisy, G.G., 2003. Cellular motility driven by assembly and disassembly of actin filaments. Cell 112, 453–465.

Pollard, T.D., Blanchoin, L., Mullins, R.D., 2000. Molecular mechanisms controlling actin filament dynamics in nonmuscle cells. Annu. Rev. Biophys. Biomol. Struct. 29, 545–576.

Ready, D.F., 2002. *Drosophila* compound eye morphogenesis: blind mechanical engineers? Results Probl. Cell Differ. 37, 191–204.

Ready, D.F., Hanson, T.E., Benzer, S., 1976. Development of the *Drosophila* retina, a neurocrystalline lattice. Dev. Biol. 53, 217–240.

Ren, N., Charlton, J., Adler, P.N., 2007. The flare gene, which encodes the AIP1 protein of *Drosophila*, functions to regulate F-actin disassembly in pupal epidermal cells. Genetics 176, 2223–2234.

Rogers, E.M., Hsiung, F., Rodrigues, A.B., Moses, K., 2005. Slingshot cofilin phosphatase localization is regulated by receptor tyrosine kinases and regulates cytoskeletal structure in the developing *Drosophila* eye. Mech. Dev. 122, 1194–1205.

Sullivan, W., Ashburner, M., Hawley, R.S., 2000. *Drosophila* Protocols. Cold Spring Harbor Laboratory Press, Cold Spring Harbor, NY.

Tepass, U., Harris, K.P., 2007. Adherens junctions in *Drosophila* retinal morphogenesis. Trends Cell Biol. 17, 26–35.

Wang, W., Eddy, R., Condeelis, J., 2007. The cofilin pathway in breast cancer invasion and metastasis. Nat. Rev., Cancer 7, 429–440.

Wolff, T., Ready, D.F., 1991. The beginning of pattern formation in the *Drosophila* compound eye: the morphogenetic furrow and the second mitotic wave. Development 113, 841–850.

Xu, T., Rubin, G.M., 1993. Analysis of genetic mosaics in developing and adult *Drosophila* tissues. Development 117, 1223–1237.

Yang, N., Higuchi, O., Ohashi, K., Nagata, K., Wada, A., Kangawa, K., Nishida, E., Mizuno, K., 1998. Cofilin phosphorylation by LIM-kinase 1 and its role in Rac-mediated actin reorganization. Nature 393, 809–8012.